

# Second Order Optimization for Adversarial Robustness and Interpretability

Theodoros Tsiligkaridis,<sup>1 †\*</sup> Jay Roberts<sup>1 †\*</sup>

<sup>1</sup> Massachusetts Institute of Technology Lincoln Laboratory

<sup>†</sup> Artificial Intelligence Technology Group, <sup>‡</sup> Homeland Sensors and Analytics Group

244 Wood St, Lexington, MA 02421

{ttsili, jay.roberts}@ll.mit.edu

## Abstract

Deep neural networks are easily fooled by small perturbations known as adversarial attacks. Adversarial Training (AT) is a technique aimed at learning features robust to such attacks and is widely regarded as a very effective defense. However, the computational cost of such training can be prohibitive as the network size and input dimensions grow. Inspired by the relationship between robustness and curvature, we propose a novel regularizer which incorporates first and second order information via a quadratic approximation to the adversarial loss. The worst case quadratic loss is approximated via an iterative scheme. It is shown that using only a single iteration in our regularizer achieves stronger robustness than prior gradient and curvature regularization schemes, avoids gradient obfuscation, and, with additional iterations, achieves strong robustness with significantly lower training time than AT. Further, it retains the interesting facet of AT that networks learn features which are well-aligned with human perception. We demonstrate experimentally that our method produces higher quality human-interpretable features than other geometric regularization techniques. These robust features are then used to provide human-friendly explanations to model predictions.

## Introduction

Deep neural networks (DNN) are powerful models that have achieved excellent performance across various domains (LeCun, Bengio, and Hinton 2015) by exploiting hierarchical representations of data. As these models are being deployed across industries, such as healthcare and autonomous driving, robustness and interpretability concerns become increasingly important. Several organizations have also identified important principles of artificial intelligence (AI) that include notions of reliability and transparency (Pichai 2018; Microsoft 2019; Lopez 2020).

One issues of such large capacity models is that small, carefully chosen input perturbations, known as adversarial perturbations, can lead to incorrect predictions (Goodfellow, Shlens, and Szegedy 2015). Various enhancement methods have been proposed to defend against adversarial perturbations (Kurakin, Goodfellow, and Bengio 2017; Ros and Doshi-Velez 2018; Madry et al. 2018; Moosavi-Dezfooli et al. 2019). One of the best performing algorithms is adversarial training (AT) (Madry et al. 2018),

which defends against strong adversarial perturbations by attacking the model during training. Computing these adversarial perturbations at each step of AT requires many iterations of a gradient-based optimization to be performed for each new minibatch. This becomes computationally prohibitive as the model size and input dimensions grow. Training against weaker attacks can reduce this cost but leads to strong robustness against weak attacks and brittleness against stronger attacks. This can be due to gradient obfuscation (Uesato et al. 2018; Athalye, Carlini, and Wagner 2018), a phenomena where networks learn to defend against gradient-based attacks by making the loss landscape highly non-linear. Another sign of gradient obfuscation is when adversarial attacks computed with a few iterations fail but black-box attacks successfully find adversarial perturbations (Uesato et al. 2018; Guo et al. 2019).

Another major concern is interpretability of DNN decisions and explanation methods for AI system users or stakeholders. Insights into model behavior based on counterfactual explanations has the potential to be very useful for users (Wachter, Mittelstadt, and Russell 2018). However, standard networks do not have interpretable saliency maps and adversarial attacks tend to be visually imperceptible. Some popular explanation methods include layerwise relevance propagation (LRP) (Bach et al. 2015), locally interpretable model-agnostic explanations (Ribeiro, Singh, and Guestrin 2016), and contrastive explanations (Dhurandhar et al. 2019), but these methods only yield feature relevance and are susceptible to spurious correlations prevalent in standard networks (Ilyas et al. 2019). The relationship between adversarial robustness and saliency map interpretability was recently studied in (Etmann et al. 2019) but experiments were based on gradient regularization. Furthermore, recent works (Tsipras et al. 2019; Ilyas et al. 2019) claim that existence of adversarial examples are due to standard training methods that rely on highly predictive but non-robust features, and make connections between robustness and explainability.

In this paper, we propose a quadratic-approximation of adversarial attacks that we incorporate into a regularizer which smooths the loss landscape and yields adversarial robustness. This smoothness implies that, in a neighborhood of a point  $x$ , the loss landscape is well approximated by gradient and curvature information. Our models avoid gradi-

\* Authors have made equal contributions.

ent obfuscation by exploiting this information. We refer to this second-order robust optimization approach as SCORPIO. We empirically show that networks trained with the SCORPIO regularizer combat gradient obfuscation and retain a high level of robustness against various types of strong attacks. Furthermore, we show how these networks improve interpretability and can be used to explain DNN predictions using a framework inspired by (Dhurandhar et al. 2019; Ilyas et al. 2019). Our main contributions are summarized below:

- A new regularizer is proposed (that may be adapted for any  $L^p$  norm) with minimal tuning parameters based on projection-free Frank-Wolfe iterations on a local quadratic-approximation to the adversarial risk that incorporates second-order information.
- It is shown that the SCORPIO regularizer trains faster than AT, provides robustness nearly on the same level as AT, and outperforms prior gradient and curvature regularizers when evaluated under various types of strong white-box attacks.
- It is demonstrated experimentally that SCORPIO better protects models against some black-box attacks than AT, suggesting that SCORPIO suffers from less gradient obfuscation than AT.
- It is shown that the quadratic-approximate attacks are still successful against robust models.
- It is shown that the quality of saliency maps and adversarial perturbations improves for the SCORPIO regularizer.

## Background and Previous Work

Consider  $(x_i, y_i) \sim \mathcal{D}$  pairs of data examples drawn from distribution  $\mathcal{D}$ . The labels are assumed to span  $K$  classes. The neural network function  $f_\theta(\cdot)$  maps input features into logits, where  $\theta$  are the model parameters. The class probability scores are obtained using the softmax transformation  $p_k(x) = e^{f_{\theta,k}(x)} / \sum_l e^{f_{\theta,l}(x)}$ . The predicted class label is given by  $\hat{y}(x) = \arg \max_k f_{\theta,k}(x)$ .

The prevalent way of training classifiers is through empirical risk minimization (ERM):

$$\min_{\theta} \mathbb{E}_{(x,y) \sim \mathcal{D}} [\ell(x, y; \theta)]$$

where the loss is the cross-entropy loss function given by  $\ell(f_\theta(x), y) = \ell(x, y; \theta) = -y^T \log(p_\theta(x))$ , where  $y$  denotes the one-hot label vector.

Adversarial robustness for a classifier  $f_\theta$  is defined with respect to a metric, here chosen as the  $L^p$  metric associated with the ball  $B_p(\epsilon) = \{\delta : \|\delta\|_p \leq \epsilon\}$ , as follows. A network is said to be robust to adversarial perturbations of size  $\epsilon$  at a given input example  $x$  iff  $\hat{y}(x) = \hat{y}(x + \delta)$  for all  $\delta \in B_p(\epsilon)$ , i.e., if the predicted label does not change for all perturbations of size up to  $\epsilon$ . The  $\epsilon$  is often referred to as the strength or budget of the attack.

Training neural networks using the ERM principle gives high accuracy on test sets, but leaves the network vulnerable to adversarial attacks. One of the most effective defenses against such attacks is adversarial training (AT) (Madry et al.

2018) which aims to minimize the adversarial risk instead,

$$\min_{\theta} \mathbb{E}_{(x,y) \sim \mathcal{D}} \left[ \max_{\delta \in B_p(\epsilon)} \ell(x + \delta, y; \theta) \right]. \quad (1)$$

The training procedure constructs adversarial attacks at given inputs  $x$  that aim to solve the inner maximization problem. Common maximization methods typically use a fixed number of gradient-ascent optimizations. One such method is projected gradient descent (PGD) that performs the iterative updates:

$$\delta^{(k+1)} = P_{B_p(\epsilon)}(\delta^{(k)} + \alpha \nabla_{\delta} \ell(x + \delta, y; \theta)) \quad (2)$$

where  $P_{B_p(\epsilon)}(z) = \arg \min_{u \in B_p(\epsilon)} \|z - u\|_2^2$  denotes the orthogonal projection onto the constraint set. The sign of the gradient has also been shown to be an effective perturbation. The computational cost of this method is dominated by the number of steps used to approximate the inner maximization, since an  $N$  step PGD approximation to the maximization (denoted PGD( $N$ )) involves  $N$  forward-backward propagations through the network. While using fewer PGD steps can lower this cost, these amount to weaker attacks which can lead to gradient obfuscation (Papernot et al. 2017; Uesato et al. 2018).

Prior works on regularization for adversarial robustness include gradient (Lyu, Huang, and Liang 2015; Ros and Doshi-Velez 2018) and curvature based penalties (Moosavi-Dezfooli et al. 2019). Gradient methods have not been shown to yield good robustness against strong attacks, while the relationship between small curvature and high robustness has been better established, but still leaves significant room for improvement. Based on the connection between curvature and robustness, a regularizer that promotes local linearity near training examples was proposed in (Qin et al. 2019) which is based on minimizing an upper bound on the adversarial risk via several PGD steps. These methods argue that flattening the decision boundary via the loss is a suitable defense against adversarial attacks.

## Approximating the Adversarial Attack

For this section we suppress the explicit dependence on the network and target and let  $\ell(x) := \ell(f_\theta(x), y)$ . Rather than approximate the maximization of (1) directly first define quadratic-approximate risk function

$$Q(v; x) := \nabla_x \ell(x) \cdot v + \frac{1}{2} v^T \nabla_x^2 \ell(x) v \quad (3)$$

and then propose solving the quadratic approximate risk optimization problem,

$$v_Q = \operatorname{argmax}_{\|v\|_p \leq \epsilon} Q(v; x). \quad (4)$$

Intuitively, we expect this quadratic approximate loss,  $\ell(x + v_Q)$  to play the role of the adversarial risk, and  $v_Q$  to play that of an attack.

In order to compare the quadratic-approximate attack and the adversarial attack we let

$$v_A = \operatorname{argmax}_{v \in B_p(\epsilon)} \ell(x + v)$$

be the optimal adversarial attack and define  $L_A = \ell(x + v_A)$  and  $L_Q = \ell(x + v_Q)$  to be the corresponding worst case adversarial-loss and the worst case quadratic-approximate loss, respectively. The following theorem gives bounds on these two losses in terms of the regularity of the loss, and so implicitly the network.

**Theorem 1.** *Let  $L_A$  and  $L_Q$  be the worst case adversarial loss and worst case quadratic-approximate loss at some  $x$  over  $B_p(\epsilon)$ . If  $\ell \circ f_\theta \in C^3(B_p(\epsilon))$  then*

$$|L_A - L_Q| \leq 2\epsilon \|\nabla_x \ell(x)\|_q + 2\epsilon^2 \|\nabla_x^2 \ell(x)\|_{p,q} + \frac{\epsilon^3 M}{3} \quad (5)$$

where  $M$  is the supremum-norm of all derivatives of  $\ell(x)$  of order three, over  $B_p(\epsilon)$ .

It is important here to emphasize the implications of Theorem 1. The amount by which the quadratic-approximate attack is **either stronger or weaker** than a full adversarial attack is controlled by the strength of the attack and by the regularity of the network. The advantage of using the quadratic-approximate attack is that the optimization (4) can be well approximated with less computation complexity than standard AT.

For  $L^2$  attacks larger attack strengths,  $\epsilon$ , can still result in imperceptible changes to the input. However,  $L^\infty$  attacks are considered stronger attacks since they can deceive a network using a smaller strength perturbation, and so modify the input in a less perceptible way. Theorem 1 suggests that the gap between the two attacks should be smaller in the  $L^\infty$  case than  $L^2$ . This is demonstrated experimentally below.

It has been shown experimentally that many robust models, including AT and the geometric-regularization methods mentioned above, have the more regular loss landscapes than their non-robust counterparts (Lyu, Huang, and Liang 2015; Ros and Doshi-Velez 2018; Moosavi-Dezfooli et al. 2019; Qin et al. 2019). Theorem 1 implies that greater regularity of the network, and thus its decision boundary, will result in a smaller gap between the quadratic approximate risk and the adversarial risk. This suggests that the quadratic approximate attacks,  $v_Q$ , should fool robust models at similar rates to PGD attacks. However, standard non-robust models can be much less regular, suggesting quadratic-approximate attacks will not perform as well as min-max attacks. We demonstrate this phenomena experimentally below.

The new approximate attack into the loss via a regularizer that penalizes deviation from the original prediction

$$\ell_Q = \ell(x + v_Q) - \ell(x). \quad (6)$$

Since  $\ell_Q = Q(v_Q) + R_{x,3}(v_Q)$ , adding it as a regularizer incorporates both gradient and curvature terms not explicitly exploited by AT. Further it does this without directly computing these derivatives, as done in gradient and curvature regularizations, which can lead to expensive backprop steps during training.

### Finding the Optimal Approximate Attack

Let  $v^k$  be the approximate solution to (4) at step  $k$ ,  $g = \nabla_x \ell(x)$ , and  $H = \nabla_x^2 \ell(x)$ . A good initialization for the iteration is  $v^0 = \epsilon g / \|g\|_p$ , since this maximizes the inner

product term; moreover, it has been demonstrated experimentally that the gradient direction is well aligned with the direction of maximum curvature of neural networks (Jetley, Lord, and Torr 2018; Fawzi et al. 2018) so  $v^0$  also serves as a strong initialization for the curvature term  $v^T H v$ .

An obvious first choice would be projected gradient descent as is done in AT, but instead of optimizing the adversarial risk we would optimize (3). However, this method involves tuning the step size  $\alpha$ , and we experimentally found that it provided less robustness than the next approach for the same number of steps.

For these reasons we use a Frank-Wolfe (FW) iteration, (Jaggi 2013). This method first solves a linearized version of the problem over convex sets,

$$\begin{cases} s^k := \operatorname{argmax}_{\|s\|_p \leq \epsilon} s \cdot \nabla_v Q(v^k) \\ v^{k+1} := (1 - \gamma^k)v^k + \gamma^k s^k \end{cases} \quad (7)$$

where  $\gamma^k = 2/(2 + k)$  is the step size. The FW sub-problem can be solved exactly for any  $L^p$  and the optimal  $s^k = P_{FW}(v^k; p)$  is given by

$$P_{FW}(v^k; p) = \alpha \cdot \operatorname{sgn}(\nabla_v Q(v^k)_i) |\nabla_v Q(v^k)_i|^{p/q} \quad (8)$$

with  $\alpha$  chosen so that  $\|s^k\|_p = \epsilon$ .

Note FW does not require a projection onto the  $L^p$  ball which is non-trivial for  $p$  not in  $\{1, 2, \infty\}$ . Another advantage of FW is the  $\gamma^k$  do not need to be tuned. Interestingly, for the special case of  $L^\infty$  attacks the optimal solution becomes the signed gradient of the quadratic approximation, i.e.  $s^k = \epsilon \operatorname{sgn}(\nabla_v Q(v^k))$ . This suggests a connection to the Fast Gradient Sign Method (FGSM) of adversarial attacks, (Goodfellow, Shlens, and Szegedy 2015).

**Proposition 1.** *If  $v^0 = g$  and  $H$  is positive-semi-definite then the sequence of  $v^k$  defined by (7) is a non-decreasing sequence for  $Q$ . That is for all  $k \geq 0$*

$$Q(v^k) \geq Q(v^{k-1}) \geq \dots \geq 0.$$

The condition that the Hessian of the loss,  $H$ , be positive semi-definite has been shown to hold locally for all  $x$ , excluding a set of measure 0, when the network uses ReLU activations and the loss is categorical cross entropy (Singla et al. 2019).

### Computational Complexity

At each iteration of FW the gradient of the quadratic approximate risk are required. The term

$$\nabla_v Q(v) = \nabla_x \ell(x) + \nabla_x^2 \ell(x)v \quad (9)$$

requires a Hessian vector product. We note that use of this gradient into (7) incorporates first- and second-order loss information into each iteration. One can compute the Hessian vector product in 1 forward and 2 backward passes. However, computing backward passes during training is expensive. Further, it was noted in (Moosavi-Dezfooli et al. 2019) that using highly localized curvature information conferred less robustness to the model and using a finite difference with relatively large step sizes allowed the network to regularize the loss curvature in a neighborhood of the sample

point. For these reasons we propose using two approximations to the Hessian vector product. First, the Forward Euler (FE) approximation

$$\nabla_x^2 \ell(x)v \approx \frac{[\nabla_x \ell(x + hv) - \nabla_x \ell(x)]}{h} \quad (10)$$

and the Central Difference (CD) approximation

$$\nabla_x^2 \ell(x)v \approx \frac{[\nabla_x \ell(x + hv) - \nabla_x \ell(x - hv)]}{2h}. \quad (11)$$

Naively, computing (9) with either finite difference costs three forward and one backward pass; however, the gradient at  $x$  can be computed once and in the case of FE it can be recycled to be used into the finite-difference term. The cost of an  $N$ -iteration FW is then  $N + 1$  forward and backward passes for FE and  $2N + 1$  for CD. The FW-FE algorithm with gradient recycling is given in Algorithm 1.

In our experiments we show that even for  $N = 3$  both FE- and CD-SCORPIO, costing 4 and 7 forward-backward passes respectively, achieve nearly the same robustness as PGD(10)-AT which costs 10 forward-backward passes.

Note that if sufficient memory is available CD can be further optimized by parallelizing the computation of the forward pass of  $x \pm hv$  allowing modern deep learning frameworks on GPU hardware to parallelize the majority of the computations. In practice on CIFAR-10 and SVHN with batch sizes of 512 we see little difference in the FE and CD training times.

---

**Algorithm 1:** Forward Euler Frank Wolfe (FE-FW) applied to a neural network  $f_\theta$ , at an input  $x_0$  with corresponding target  $y_0$  and a loss  $\ell$ .

---

**Input :**  $N, \epsilon, h, p$   
**Output:** Approximate solution,  $v^*$ , to (4).

```

1  $l^0 = \ell(f_\theta(x_0), y_0)$ 
2  $g^0 = \mathbf{grad}[l^0, x_0]$ 
3  $v^* \leftarrow g^0$ 
4 for  $k \in \{0, \dots, N - 1\}$  do
5    $\gamma^k = 2/(2 + k)$ 
6    $l^k = \ell(f_\theta(x_0 + hv^*), y_0)$ 
7    $g^k = \mathbf{grad}[l^k, x_0]$ 
8    $s^k = \epsilon * F_{FW}(g^0 + \frac{1}{h}(g^k - g^0); p)$ 
9    $v^* \leftarrow (1 - \gamma^k)v^* + \gamma^k s^k$ 
10 end
```

---

## Experimental Results

We evaluate the performance of our proposed SCORPIO regularizer against standard networks, gradient regularized networks (Grad-Reg) (Ros and Doshi-Velez 2018), curvature regularized networks (CURE) (Moosavi-Dezfooli et al. 2019), and adversarial training (AT) (Madry et al. 2018).

### Implementation

The models, training, and evaluation routines for our experiments were performed using the robustness library from

(Engstrom et al. 2019) which we modified to support the SVHN dataset. Experiments were run on 2 Volta V100 GPUs using the computing resources at (**Computing credits censored to maintain anonymity**).

Hyperparameters were tuned for each experiment with the goal of achieving near the clean accuracy of AT. For SCORPIO models, the finite difference step size  $h$  and regularization strength  $r$  were tuned via a manual search for both between 0.5 and 1.5. For tuning CURE, grad-reg, we chose the regularization strength to be as large as possible while still nearly matching the clean accuracy of AT. For AT we ran PGD with 10 steps and chose the best model that achieves the highest adversarial accuracy at  $\epsilon = 0.5$  for  $L^2$  robustness and  $\epsilon = 8/255.0$  for  $L^\infty$  robustness. Specifics can be found in the supplementary materials.

### Adversarial Robustness

To test the robustness of our network, we consider a variety of adversarial attacks, including untargeted and targeted attacks towards a random class  $r \sim \text{Unif}(\{1, \dots, K\} \setminus y)$ . The classification margin is defined as:

$$M(x, y) = \log p_y(x) - \max_{j \neq y} \log p_j(x) \quad (12)$$

The following loss functions are used to obtain low adversarial accuracy:

**(UL) Untargeted-loss:**  $\max_{\delta \in B(\epsilon)} l(x + \delta, y)$

**(TL) Rand. Targeted-loss:**  $\max_{\delta \in B(\epsilon)} l(x + \delta, r)$

**(UM) Untargeted-margin:**  $\min_{\delta \in B(\epsilon)} M(x + \delta, y)$

**(TM) Rand. Targeted-margin:**  $\max_{\delta \in B(\epsilon)} M(x + \delta, r)$

The performance metric used is the accuracy on the test set after the attack is applied, i.e., adversarial accuracy. We empirically observed that the margin-based attacks on robust models are stronger than loss-based attacks for robust models.

On CIFAR-10 SCORPIO outperforms both Grad-Reg and CURE by a sizable margin and achieves robustness close to that of AT for increasingly strong attacks. The gap between SCORPIO and AT is smaller for the  $L^\infty$  case than the  $L^2$ , see Figure 1a and 1b. In Table 2a and 2b we report results for the specific attacks in the  $L^2$  and  $L^\infty$  case, respectively. In general untargeted attacks are stronger than targeted and margin attacks are stronger than loss based ones. For all attacks the trend holds that SCORPIO outperforms the geometric regularizers and is close to AT.

The SVHN dataset followed the same trends. In all cases SCORPIO outperforms Grad-Reg and CURE and is close to, sometimes better than, AT. see Figure 1c and 1d and supplemental tables 7a and 7b for details.

### Approximate Quadratic Attacks

For these experiments we compare  $L^2$  PGD adversarial attacks on the loss against the quadratic-approximate attacks obtained by approximating solutions to (4). We compute adversarial attacks using  $N = 10$  PGD steps and approximate the quadratic-approximate attacks with  $N = 3$  steps of Frank-Wolfe (FE). We see for models with smoother

Method	Clean	PGD(10)	PGD(20)	PGD(40)	PGD(100)
SCORPIO (FE,N=1)	<b>89.42</b>	<b>66.35</b>	<b>66.06</b>	<b>65.98</b>	<b>65.97</b>
SCORPIO (CD,N=1)	<b>88.16</b>	<b>66.03</b>	<b>65.83</b>	<b>65.74</b>	<b>65.72</b>
Adv Train (PGD-3)	87.62	63.19	62.89	62.81	62.81

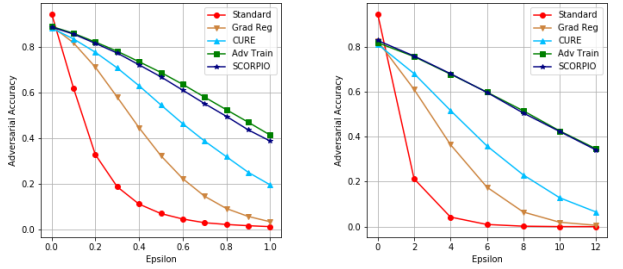
Table 1: Model accuracy on CIFAR-10 test set for untargeted margining (UM) based adversarial  $L^2$  PGD attacks on the margin at  $\epsilon = 0.5$  for robust networks trained against  $L^2$  adversary. The step size for PGD was set to  $\alpha = 0.1$ . Both methods are trained starting from pretrained standard networks with fine-tuning. Our proposed regularizer, SCORPIO, with one FW step  $N = 1$ , outperforms the PGD-based adversarial training with  $N = 3$  steps.

Method	Clean	UL	TL	UM	TM
Standard	94.5	6.9	27.3	6.6	29.4
Gradient Reg	89.2	32.3	70.2	32.2	66.9
CURE	88.3	54.6	81.5	53.7	79.5
SCORPIO (FE,N=3)	88.7	66.9	85.3	66.8	83.8
SCORPIO (CD,N=3)	89.9	66.4	85.4	66.2	83.8
Adv Train (PGD-10)	89.0	68.8	85.4	68.8	84.6

(a)  $L^2$  adversarial PGD(10) attacks with loss / margin at  $\epsilon = 0.5$

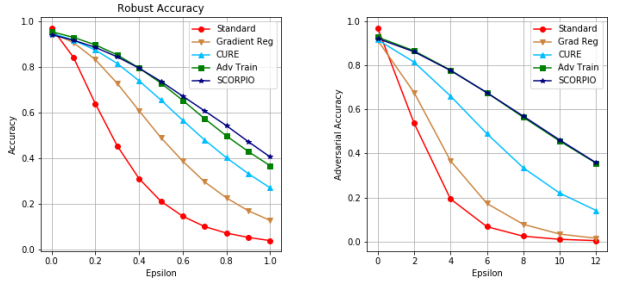
Method	Clean	UL	TL	UM	TM
Standard	94.5	0.2	13.2	0.3	14.4
Gradient Reg	82.5	6.5	40.0	7.1	34.8
CURE	81.1	23.0	60.7	22.4	54.3
SCORPIO (FE,N=3)	82.7	50.5	75.2	48.7	73.0
SCORPIO (CD,N=3)	83.3	49.2	74.6	47.2	71.9
Adv Train (PGD-10)	81.7	51.5	75.1	49.9	72.7

(b)  $L^\infty$  adversarial PGD(10) attacks with loss / margin at  $\epsilon = 8/255$



(a) CIFAR10  $L^2$  robustness.

(b) CIFAR10  $L^\infty$  robustness.



(c) SVHN  $L^2$  robustness.

(d) SVHN  $L^\infty$  robustness.

Figure 1: Adversarial accuracy as a function of  $\epsilon$  on CIFAR-10 (a,b) and SVHN (c,d) test set. Adversarial attacks on the loss using PGD(10) were used for evaluating robustness. We observe SCORPIO-FE(3) achieves nearly the same robustness levels as adversarial training with PGD(10) adversary and outperforms gradient and curvature regularizers by a large margin.

Figure 2: Model accuracy on CIFAR-10 test set against various attacks. Our proposed regularizer, SCORPIO, outperforms prior gradient and curvature regularization methods achieves nearly the same level of robustness as AT in all cases.

loss surfaces, AT, SCORPIO, and CURE, the quadratic-approximate attack performs as well or better than traditional adversarial attacks. However, for standard models PGD attacks are superior than the quadratic-approximate attack. Based on Theorem 1 we believe this is a demonstration of the quadratic-approximate attack’s ability to exploit regularized decision boundaries which are not present in standard models.

We emphasize that although quadratic-approximate attacks are not as strong as PGD against standard models, training standard models with the proposed SCORPIO regularizer none-the-less confers strong robustness as shown above.

## Evaluating Gradient Masking

We evaluate gradient masking by following a similar evaluation protocol as in (Moosavi-Dezfooli et al. 2019) inspired by (Uesato et al. 2018). Table 1 shows that our method achieves similar adversarial accuracy on the test set when evaluated against stronger PGD attacks. Thus increasing the attack’s complexity does not deteriorate the adversarial accuracy significantly. Furthermore, we evaluate our model

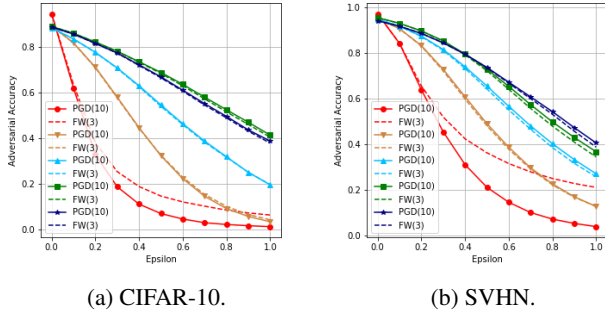


Figure 3: Comparison between adversarial risk attacks (solid lines) and the quadratic-approximate risk attacks (dashed lines) on CIFAR-10 (right) and SVHN (left) datasets for varying strength  $L^2$  attacks. Quadratic approximate attacks are slightly more successful than adversarial attacks on robust models (green, purple, blue, orange) but much less successful against standard models (red) likely due to these models having less regular decision boundaries.

against black box gradient-free method SimBA (Guo et al. 2019), and compared the margin computed using SimBA and PGD for a large batch of test points in Figure 4a and 4b and observe that both methods lead to a similar adversarial loss except on a very small subset of points (12 out of 1000) for SCORPIO which improves upon the number of red points for AT (29 out of 1000). Here, the adversarial loss corresponds to the classification margin which captures the confidence in correct classifications and is positive for correct predictions and negative for misclassifications. This further verifies that our proposed method improves the true robustness and does not suffer from gradient masking or obfuscation.

### Interpretability

We compare the quality of the saliency maps generated with a variety of regularized networks, in addition to adversarial perturbations that can serve as counterfactuals for explanations. We note that standard networks produce very noisy saliency maps, as previously noted (Etmann et al. 2019), and the higher level of robustness a network exhibits the more the network focuses on the object semantics as shown in Figure 5a. The counterfactual images generated in Figure 5b using (13) align better with human perception for our method than for gradient and curvature regularized models.

Figures 6b and 6a show example images from the CIFAR-10 test set, out of which the first three columns correspond to correct classifications and the last two columns correspond to misclassifications. Although saliency maps for our model focus more on the object of interest, identify areas in the image that most influence the predictions, and are a good sign of lack of gradient obfuscation (Qin et al. 2019), they cannot be directly used to reason about what features and how would need to change to correct a misclassification or how to justify a misclassification or a correct prediction.

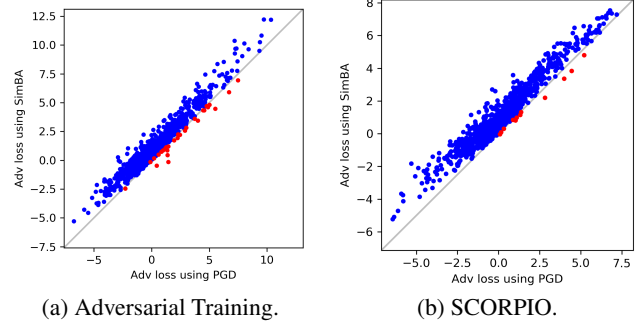
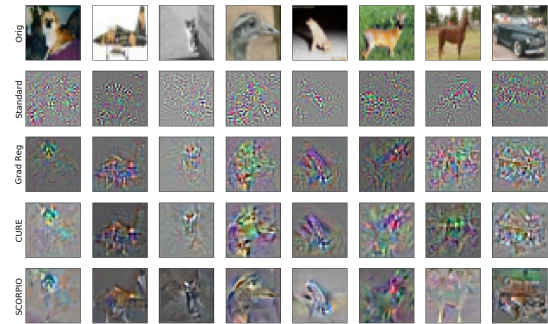
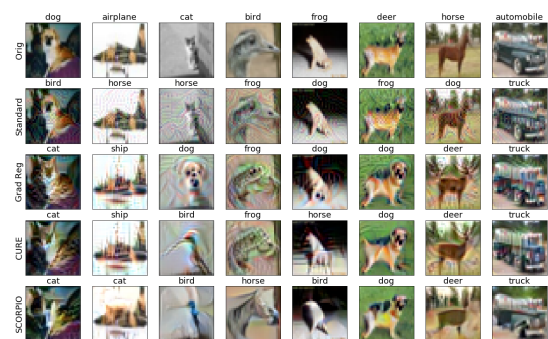


Figure 4: Gradient masking analysis for network trained with adversarial training PGD(10) and SCORPIO- $L^\infty$ . Adversarial loss here refers to the logit difference/margin (12) and was computed with SimBA ( $T = 200$ ,  $\epsilon = 0.2$ ) for the y-axis and PGD(100) at  $\epsilon = 8/255$  for x-axis on a set of 1000 test points. Points near the line  $y = x$  indicate both types of attacks found similar adversarial perturbations, while points below the line shown in red imply that SimBA identified stronger attacks than PGD. SCORPIO exhibits a higher resistance to gradient masking.



(a) Saliency Maps.



(b) Adversarial Perturbations.

Figure 5: Saliency maps and PGD(20) untargeted adversarial attacks on the loss for sample examples from CIFAR-10 test set. We observe that our method SCORPIO achieves more realistic-looking adversarial perturbations and the quality of the saliency maps improves.

To this end, we consider a framework inspired by contrastive explanations (Dhurandhar et al. 2019) and the robust feature manipulation by (Tsipras et al. 2019). Without loss of generality, we consider explaining decisions of an  $L^2$ -robust network<sup>1</sup>. Our approach seeks to find *pertinent negatives/positives* by optimizing over the perturbation variable  $\delta$  that is used to explain the prediction. Pertinent negatives capture what is missing in the prediction, and pertinent positives refer to critical features that are present in the input examples.

Suppose we have  $(x, y) \sim \mathcal{D}$ , then we consider two contrastive explanations defined by the optimizations

$$\delta_{\max} := \operatorname{argmax}_{\delta \in B_2(\epsilon)} l(x + \delta, y) \quad (13)$$

and

$$\delta_{\min} := \operatorname{argmin}_{\delta \in B_2(\epsilon)} l(x + \delta, y), \quad (14)$$

we optimize the loss over a  $L^2$  ball of radius  $\epsilon$  to ensure that the modified example  $x + \delta_m$  remains close to the original example  $x$  in both cases.

In the case of correct predictions  $\delta_{\max}$  are the features within, or that could be added to, the original image which would flip the network’s decision to a nearby class so are *pertinent negative features* of the image. Whereas,  $\delta_{\min}$  are the features which contribute to the correct prediction, making them the *pertinent positive features*. In the case of incorrect predictions the roles are flipped. The roles are summarized below.

Pred.	$\delta_{\max}$	$\delta_{\min}$
correct	PP	PN
incorrect	PN	PP

For example consider the correct prediction in column 2 of Figure 6a and 6b. The network correctly predicts the image is of a ship and the pertinent positive features,  $\delta_{\min}$ , are emphasizing the mast and box of the ship. The pertinent negative features,  $\delta_{\max}$ , show a nearby class for this image of a ship is airplane, but the features that need to be added to the original image in order to make it predict airplane are wings and shorter tail. Part of the explanation for this ship label is the *absence* of these airplane features.

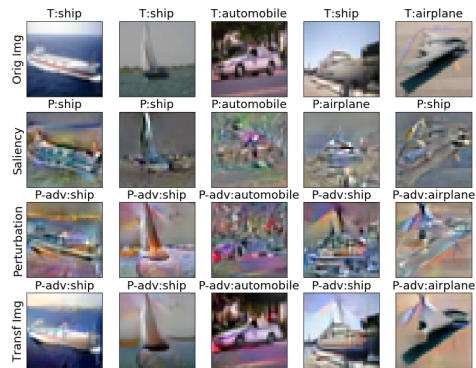
For an incorrect example consider column 4 of of Figure 6a and 6b. The network incorrectly predicts the image of a ship is an airplane. The  $\delta_{\max}$  is now encoding the pertinent positive features and we see the perturbation emphasizes a portion at the bottom of the image which resembles landing gear. The pertinent negative features, now  $\delta_{\min}$  suggest that the image lacks a clear distinction between the deck and hull and between the dock and water. As the transformed image  $x + \delta_{\min}$  shows, the introduction of mast and mainsail features would correct this error. We remark that other elements in the image such as the sky and background are minimally perturbed.

These contrastive explanations coupled with adversarial learning have many potential uses such as: detect bias in

<sup>1</sup> This can be extended to  $L^\infty$  as well, as we have noticed similar trends for robust models against  $L^\infty$  adversaries.



(a)  $\delta_{\max}$  Perturbations.



(b)  $\delta_{\min}$  Perturbations.

Figure 6: Contrastive explanations with SCORPIO on CIFAR-10 dataset. The perturbations were generated by solving (14) and (13) via PGD with  $\epsilon = 4$  and 20 steps.

training datasets, diagnose common errors made by a network, or distill concepts learned by the network, to name a few.

## Conclusion

One of the most popular and effective training algorithms for robustness is adversarial training (AT), but is computationally expensive and does not incorporate curvature information into its attacks. We propose an approximate attack based on the quadratic-approximation to the adversarial risk that we show mathematically results in a worst case loss near the optimal adversarial loss. The attack is implemented via a Frank Wolfe iteration, which does not require projections or additional hyperparameter tuning, and a finite difference approximation that allows computing an effective quadratic approximate attack in less than half the number of forward-backward passes as AT reducing the training time. We incorporate these approximate attacks into a regularizer (SCORPIO) and demonstrate robustness near that of AT. Further, SCORPIO suffers from less gradient obfuscation than AT and the quadratic-approximate attacks are shown to be as strong as PGD attacks against regularized models. Further, we use these robust models to develop an explanation framework based on pertinent positive/negative features.

## References

- Athalye, A.; Carlini, N.; and Wagner, D. 2018. Obfuscated Gradients Give a False Sense of Security: Circumventing Defenses to Adversarial Examples. In *ICML*.
- Bach, S.; Binder, A.; Montavon, G.; Klauschen, F.; Muller, K.-R.; and Samek, W. 2015. On pixel-wise explanations for non-linear classifier decisions by layer-wise relevance propagation. *PLoS one* 10(7).
- Dhurandhar, A.; Chen, P.-Y.; Luss, R.; Tu, C.-C.; Ting, P.; Shanmugam, K.; and Das, P. 2019. Explanations based on the Missing: Towards Contrastive Explanations with Pertinent Negatives. In *NeurIPS*.
- Engstrom, L.; Ilyas, A.; Santurkar, S.; and Tsipras, D. 2019. Robustness (Python Library). URL <https://github.com/MadryLab/robustness>.
- Etmann, C.; Lunz, S.; Maass, P.; and Schonlieb, C.-B. 2019. On the Connection Between Adversarial Robustness and Saliency Map Interpretability. In *ICML*.
- Fawzi, A.; Moosavi-Dezfooli, S.-M.; Frossard, P.; and Soatto, S. 2018. Empirical study of the topology and geometry of deep networks. In *CVPR*.
- Goodfellow, I. J.; Shlens, J.; and Szegedy, C. 2015. Explaining and Harnessing Adversarial Examples. In *International Conference on Learning Representations*.
- Guo, C.; Gardner, J. R.; You, Y.; Wilson, A. G.; and Weinberger, K. Q. 2019. Simple Black Box Adversarial Attacks. In *ICML*.
- Ilyas, A.; Santurkar, S.; Tsipras, D.; Engstrom, L.; Tran, B.; and Madry, A. 2019. Adversarial Examples are not Bugs, They are Features. In *NeurIPS 2019*.
- Jaggi, M. 2013. Revisiting Frank-Wolfe: Projection-Free Sparse Convex Optimization. volume 28 of *Proceedings of Machine Learning Research*, 427–435. Atlanta, Georgia, USA: PMLR. URL <http://proceedings.mlr.press/v28/jaggi13.html>.
- Jetley, S.; Lord, N.; and Torr, P. 2018. With friends like these, who needs adversaries? In *NeurIPS*.
- Kurakin, A.; Goodfellow, I. J.; and Bengio, S. 2017. Adversarial Machine Learning at Scale. In *International Conference on Learning Representations*.
- LeCun, Y.; Bengio, Y.; and Hinton, G. 2015. Deep Learning. *Nature* 521(7533): 436–444.
- Lopez, C. T. 2020. *DOD Adopts 5 Principles of Artificial Intelligence Ethics*. URL <https://www.defense.gov/Explore/News/Article/Article/2094085/dod-adopts-5-principles-of-artificial-intelligence-ethics/>.
- Lyu, C.; Huang, K.; and Liang, H.-N. 2015. A unified gradient regularization family for adversarial examples. In *IEEE International Conference on Data Mining (ICDM)*.
- Madry, A.; Makelov, A.; Schmidt, L.; Tsipras, D.; and Vladu, A. 2018. Towards Deep Learning Models Resistant to Adversarial Attacks. In *International Conference on Learning Representations*. URL <https://openreview.net/forum?id=rJzIBfZAb>.
- Microsoft. 2019. *Microsoft AI principles*. URL <https://www.microsoft.com/en-us/ai/responsible-ai>.
- Moosavi-Dezfooli, S.-M.; Uesato, J.; Fawzi, A.; and Frossard, P. 2019. Robustness via curvature regularization, and vice versa. In *IEEE Conference on Computer Vision and Pattern Recognition*. URL [https://openaccess.thecvf.com/content\\_CVPR\\_2019/papers/Moosavi-Dezfooli\\_Robustness\\_via\\_Curvature\\_Regularization\\_and\\_Vice\\_Versa\\_CVPR\\_2019\\_paper.pdf](https://openaccess.thecvf.com/content_CVPR_2019/papers/Moosavi-Dezfooli_Robustness_via_Curvature_Regularization_and_Vice_Versa_CVPR_2019_paper.pdf).
- Papernot, N.; McDaniel, P.; Goodfellow, I.; Jha, S.; Celik, Z. B.; and Swami, A. 2017. Practical Black-Box Attacks against Machine Learning. In *arXiv:1602.02697v4*.
- Pichai, S. 2018. *AI at Google: our principles*. URL <https://www.blog.google/technology/ai/ai-principles/>.
- Qin, C.; Martens, J.; Gowal, S.; Krishnan, D.; Dvijotham, K.; Fawzi, A.; De, S.; Stanforth, R.; and Kohli, P. 2019. Adversarial Robustness through Local Linearization. In *NeurIPS*.
- Ribeiro, M.; Singh, S.; and Guestrin, C. 2016. why should i trust you? explaining the predictions of any classifier. In *ACM SIGKDD Intl. Conference on Knowledge Discovery and Data Mining*.
- Ros, A. S.; and Doshi-Velez, F. 2018. Improving the Adversarial Robustness and Interpretability of Deep Neural Networks by Regularizing Their Input Gradients. In *AAAI Conference on Artificial Intelligence*.
- Singla, S.; Wallace, E.; Feng, S.; and Feizi, S. 2019. Understanding Impacts of High-Order Loss Approximations and Features in Deep Learning Interpretation.
- Tsipras, D.; Santurkar, S.; Engstrom, L.; Turner, A.; and Madry, A. 2019. Robustness May Be at Odds with Accuracy. In *International Conference on Learning Representations*. URL <https://openreview.net/forum?id=SyxAb30cY7>.
- Uesato, J.; O’Donoghue, B.; van den Oord, A.; and Kohli, P. 2018. Adversarial Risk and the Dangers of Evaluating Against Weak Attacks. In *ICML*.
- Wachter, S.; Mittelstadt, B.; and Russell, C. 2018. Counterfactual Explanations without Opening the Black Box: Automated Decisions and the GDPR. *Harvard Journal of Law & Technology* 31(2).

## Supplementary Material

### Proof of Theorem 1

*Proof.* Let  $L_A$ ,  $L_Q$ , and  $x$  be as stated in Theorem 1. Further let  $v_A$  and  $v_Q$  be the corresponding adversarial and quadratic-approximate attacks, respectively. Notice  $L_A - L_Q = \ell(x + v_A) - \ell(x) - (\ell(x + v_Q) - \ell(x))$ . Then by Taylor’s Theorem there are degree 3 polynomials,  $R_{x,3}(v_A)$  and  $R_{x,3}(v_Q)$  so that

$$\begin{aligned} L_A - L_Q &= \ell(x + v_A) - \ell(x) - (\ell(x + v_Q) - \ell(x)) \\ &= Q(v_A) - Q(v_Q) + R_{x,3}(v_A) - R_{x,3}(v_Q). \end{aligned}$$

Where we have suppressed the quadratic’s dependence on  $x$ , i.e.,  $Q(v) := Q(v; x)$ . Letting  $g = \nabla_x \ell(x)$  and  $H = \nabla_x^2 \ell(x)$  we can write the difference of the quadratics as

$$\begin{aligned} Q(v_A) - Q(v_Q) &= \langle v_A, g + \frac{1}{2} H v_A \rangle - \langle v_Q, g + \frac{1}{2} H v_Q \rangle \\ &= \langle v_A - v_Q, g \rangle + \langle v_A, \frac{1}{2} H v_A \rangle - \langle v_Q, \frac{1}{2} H v_Q \rangle \\ &= \langle v_A - v_Q, g \rangle + \langle v_A - v_Q, \frac{1}{2} H v_A \rangle \\ &\quad + \langle v_Q, \frac{1}{2} H v_A \rangle - \langle v_Q, \frac{1}{2} H v_Q \rangle \\ &= \langle v_A - v_Q, g \rangle + \langle v_A - v_Q, \frac{1}{2} H (v_A + v_Q) \rangle \end{aligned}$$

After taking the absolute value and applying the triangle inequality the gradient term is easily bounded with Holder, for the remaining

quadratic term

$$\begin{aligned} |\langle v_A - v_Q, \frac{1}{2}H(v_A + v_Q) \rangle| &\leq \frac{1}{2}|v_A - v_Q|_p \\ &\quad \times (|Hv_Q|_q + |Hv_A|_q) \\ &\leq \epsilon^2 \|H\|_{p,q}. \end{aligned}$$

Therefore,

$$|L_M - L_Q| \leq 2\epsilon|g|_q + 2\epsilon^2 \|H\|_{p,q} + |R_{x,3}(v_A)| + |R_{x,3}(v_Q)|.$$

The bound on the remainder terms is a result of Taylor’s Theorem  $\square$

## Proof of Proposition 1

Assume the conditions of Proposition 1

*Proof.* Notice that  $Q(g) \geq \frac{1}{2}g^t H g \geq 0$ . Let  $k \geq 1$  and write  $v^{k+1} = v^k + \gamma^k(s^k - v^k)$ . Then since  $Q$  is quadratic it agrees with its second order Taylor expansion about  $v^k$  and so

$$\begin{aligned} Q(v^{k+1}) - Q(v^k) &= \gamma^k \nabla_v Q(v^k) \cdot (s^k - v^k) \\ &\quad + \frac{(\gamma^k)^2}{2} (s^k - v^k)^T H (s^k - v^k) \\ &\geq \gamma^k \nabla_v Q(v^k) \cdot (s^k - v^k). \end{aligned}$$

The result follows by optimality of  $s^k$ .  $\square$

## Hyperparameters

**CIFAR-10.** For the  $L^2$  experiments the finite difference step and regularization strength,  $(h,r)$ , used were: (1.15, 1.05) for FE(3) and FE(1), (0.95, 0.999) and (1.25, 0.999) for CD(3) and CD(1). For the  $L^\infty$  experiments: (1.05, 1.05) and (0.95, 1.05) for FE(3) and FE(1), (0.95, 1.15) for both CD(3) and CD(1). The learning rate was initialized at 0.01 and decayed to 0.001 after 50 epochs. Models were trained for 60 epochs.

**SVHN.** We tested only FE difference schemes with  $N = 3$  as these were the best performers in the CIRFAR-10 experiments. The models were trained for 40 epochs with an initial learning rate of 0.01 that decayed by a factor of 10 every 8 epochs. The best model was chosen from all epochs. For the  $L^2$  experiments  $h$  was 1.25 and  $r$  was 0.99. For the  $L^\infty$  the optimal  $h$  was 1.5 and  $r$  was 1.25.

## SVHN Results

The trends seen in the CIFAR results are mirrored here in the SVHN experiments. Table 7a and 7b show that SCORPIO outperforms all geometric regularization methods and is nearly as robust, and some cases more so, than AT. We again see that untargeted attacks are stronger than targeted and that margin are somewhat stronger than loss attacks.

Method	Clean	UL	TL	UM	TM
Standard	97.0	21.2	45.6	20.7	45.8
Gradient Reg	95.0	49.1	76.0	48.2	74.3
CURE	94.7	65.5	85.6	63.9	84.3
SCORPIO (FE,N=3)	94.0	73.7	89.1	71.3	87.7
Adv Train (PGD-10)	95.3	72.9	89.0	71.7	88.2

(a)  $L^2$  adversarial PGD(10) attacks with loss / margin at  $\epsilon = 0.5$

Method	Clean	UL	TL	UM	TM
Standard	97.0	2.4	18.8	2.4	20.5
Gradient Reg	91.4	7.8	30.7	8.1	28.8
CURE	91.6	33.5	59.9	30.9	56.1
SCORPIO (FE,N=3)	92.2	56.9	77.4	52.2	73.7
Adv Train (PGD-10)	92.8	56.4	77.0	52.5	74.2

(b)  $L^\infty$  adversarial PGD(10) attacks with loss / margin at  $\epsilon = 8/255$

Figure 7: Model accuracy on SVHN test set against various attacks. Our proposed regularizer, SCORPIO, outperforms prior gradient and curvature regularization methods achieves nearly the same level of robustness as AT in all cases.